Nuclear Engineering and Technology 48 (2016) 228–235

Available online at ScienceDirect

Nuclear Engineering and Technology

journal homepage: www.elsevier.com/locate/net

Original Article

Simulation Based Investigation of Focusing Phased Array Ultrasound in Dissimilar Metal Welds

Hun-Hee Kim [a], *Hak-Joon Kim* [b,*], *Sung-Jin Song* [b], *Kyung-Cho Kim* [c], *and Yong-Buem Kim* [c]

[a] *Doosan Heavy Industries & Construction Co, Changwon 642-792, South Korea*
[b] *School of Mechanical Engineering, Sungkyunkwan University, Suwon 440-746, South Korea*
[c] *Korea Institute of Nuclear Safety, Daejeon 305-338, South Korea*

ARTICLE INFO

Article history:
Received 27 April 2015
Received in revised form
2 October 2015
Accepted 5 October 2015
Available online 2 December 2015

Keywords:
Dissimilar Metal Welds
Focusing Ultrasound
Phased Array Ultrasound

ABSTRACT

Flaws at dissimilar metal welds (DMWs), such as reactor coolant systems components, Control Rod Drive Mechanism (CRDM), Bottom Mounted Instrumentation (BMI) etc., in nuclear power plants have been found. Notably, primary water stress corrosion cracking (PWSCC) in the DMWs could cause significant reliability problems at nuclear power plants. Therefore, phased array ultrasound is widely used for inspecting surface break cracks and stress corrosion cracks in DMWs. However, inspection of DMWs using phased array ultrasound has a relatively low probability of detection of cracks, because the crystalline structure of welds causes distortion and splitting of the ultrasonic beams which propagates anisotropic medium. Therefore, advanced evaluation techniques of phased array ultrasound are needed for improvement in the probability of detection of flaws in DMWs. Thus, in this study, an investigation of focusing and steering phased array ultrasound in DMWs was carried out using a time reversal technique, and an adaptive focusing technique based on finite element method (FEM) simulation. Also, evaluation of focusing performance of three different focusing techniques was performed by comparing amplitude of phased array ultrasonic signals scattered from the targeted flaw with three different time delays.

1. Introduction

Dissimilar metal welding (DMW) is used to join stainless steel components to steel tubes in power plants. In particular, in nuclear power plants, DMWs are used in major components such as CRDM, BMI, and inlet and outlet nozzles, etc. However, primary water stress corrosion cracks (PWSCCs) have been found in DMW areas of major components in nuclear power plants. Also, Bamford and Hall [1] reviewed and compared the behavior of weldings as opposed to base metal, from the

* *Corresponding author.*
E-mail address: hjkim21c@skku.edu (H.-J. Kim).

http://dx.doi.org/10.1016/j.net.2015.10.011
1738-5733/Copyright © 2015, Published by Elsevier Korea LLC on behalf of Korean Nuclear Society.

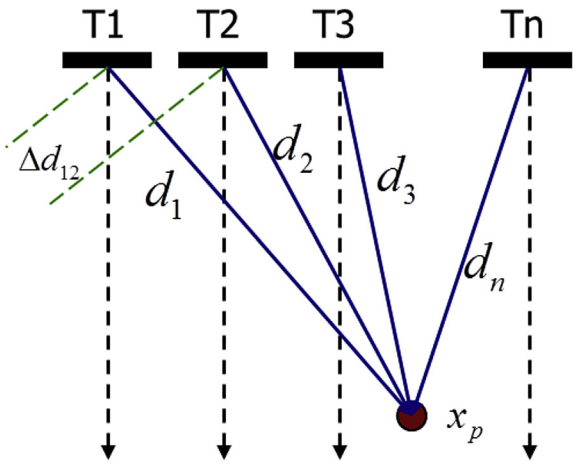

Fig. 1 – Geometry of the phased array used in deriving the focusing formula.

standpoint of time to crack initiation, growth rate of cracks, and their impact on structural integrity of nuclear power plants. Other researchers indicated that under some conditions the flaws found may lead to rupture before detectable leakage [2]. Thus, detection of PWSCC in DMWs is one of the major issues for ensuring safety of nuclear power plants. Currently, phased array ultrasound is widely used for PWSCCs and surface breaking cracks in the nuclear power plants. However, inspection of DMW using phased array ultrasound has a relatively low probability of detection of cracks, because the crystalline structure of welds causes distortion and splitting of the ultrasonic beams which propagates anisotropic medium [3]. Therefore, advanced evaluation techniques of phased array ultrasound are needed to improve the probability of detection of flaws in DMWs. Many studies have therefore been reported on DMW modeling and phased array focusing techniques to improve flaw detectability. Several studies have simulated the ultrasonic beam propagation in DMWs using an analytical method called the Athena and Mina code [4–8]. Also, Ye et al [6,7] present a model for predicting the ultrasonic beam propagation in DMWs using a modified Ogilvy's model. Other studies have simulated the ultrasonic beam propagation in DMWs using a numerical method which utilizes finite element method (FEM) software [9–11]. In order to have precise inspection of a DMW, focusing techniques of phased array ultrasound are needed to improve the probability of detection of flaws in DMWs. Recently; many studies have investigated focusing techniques using phased array ultrasonic testing. Among focusing techniques, adaptive focusing techniques and time reversal techniques are widely used to calculate time delay for focusing in anisotropic inhomogeneous materials. But these studies are limited by relative results only. Thus, in this study, a FEM model based investigation of focusing and steering ultrasonic beams in DMWs through understanding of propagation of ultrasonic waves in anisotropic inhomogeneous medium was performed. Also, the focusing performance of adaptive focusing, time reversal, and conventional techniques in the DMWs are compared.

2. Methods

2.1. Focusing techniques

2.1.1. Conventional focusing techniques

A phased array transducer consists of individual elements that are composed of piezoelectric crystals. To focus the phased array ultrasonic beam, time delays are applied to the array elements. In order to determine the time delay, the distance of each element to the focal spot should be identified. Fig. 1 shows a schematic diagram of the conventional focusing technique. T_1, T_2 and T_n in Fig. 1 indicate phased array elements which generate an ultrasonic beam. Then, the time delay can be determined using Equations 1 and 2.

$$P_{t_n} = Ae^{ikd_n}e^{-i\omega t} \tag{1}$$

where, P_{t1}, P_{t2}, and P_{tn} are radiated sound pressure by the n-th phased array elements (T_1, T_2 and T_n) at the interrogation point (x_p), as shown in Fig. 1. A is the input amplitude from the phased array elements; d_1, d_2 and d_n are the distances between the phased array element and the inspection point. For phase matching at point x_p, sound pressure which is T_1 and T_2 need to match using Equation 2. Δd_{12} is the gap between d_1 and d_2, C is the sound velocity of the material, and Δt_{12} is the time delay. Then, radiated sound pressure can be matched by adding a time delay, defined in Equation 3.

$$\exp[ikd_1] = \exp[ikd_2]\exp[ik\Delta d_{12}] = \exp[ikd_2]\exp[i\omega\Delta t_{12}] \tag{2}$$

$$\Delta t_{12} = \frac{\Delta d_{12}}{C} \tag{3}$$

2.1.2. Adaptive focusing techniques

The adaptive focusing technique is a time delay estimation method based on cross correlation. Cross correlation is widely used to determine the time delay through various received signals. One can calculate time delay using cross correlation between two signals acquired by two elements. Time delay can be rapidly detected and quantified using a cross correlation between each received signal, where the cross correlation function between received signals S_1 and S_2 is

$$\Delta t_n = \sum_{n=1}^{N} \max\left(\sum_{0}^{t} S_{n+1}(t-\tau)S_n(t)\right) \tag{4}$$

From each correlation function, we estimate the time delay that is obtained from the conventional cross correlation method.

For calculating the cross correlation between each received signal shown in Fig. 2A, the maximum value of the cross-correlation function indicates the point in time where the signals as best aligned, as shown in Fig. 2B.

2.1.3. Time reversal focusing techniques

The time reversal technique is a time delay estimation method that can be used in ultrasonic testing to improve flaw detection through anisotropy and inhomogeneous material such as DMWs. Among the techniques, the DORT method (French acronym for decomposition of the time reversal operator) is applied in this study. First, received signals are measured by

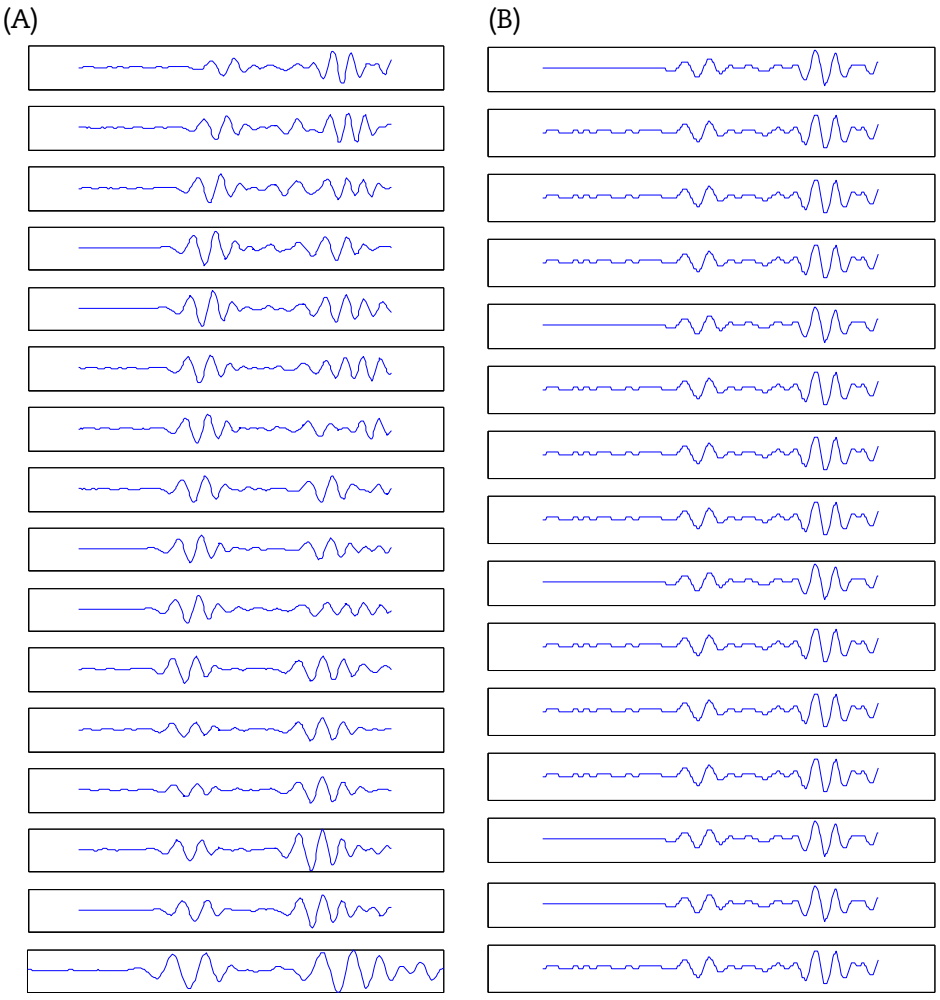

Fig. 2 – (A) Received signals and (B) aligned received signals from 16 phased array elements.

each of the elements. Then, time-domain signals are converted into frequency-domain, and singular value decomposition (SVD) of the transfer matrix is applied to obtain an eigenvalue and eigenvector as shown in Equation 5 [12]. The transfer matrix $\mathbf{K}(\omega)$ is obtained by taking the Fourier transformation into the response. The columns of V are eigenvectors of $\mathbf{K}(\omega)^*\mathbf{K}(\omega)$. The columns of U are eigenvectors of $\mathbf{K}(\omega)\mathbf{K}(\omega)^*$. The columns S^t are a diagonal positive semidefinite matrix. In practice, SVD of the transfer matrix to obtain the eigenvalue and eigenvector is used. The number of significant eigenvalues is equal to the number of well resolved scatters. And, each eigenvector provides phase and amplitude information that should be applied to the transducer array in order to focus on each scatterer. In Fig. 3, one large eigenvalue means that there is only one scatter in the sector. Fig. 4 shows that the eigenvector of the time reversal operator includes phase information.

$$\mathbf{K}(\omega) = \mathbf{U}\mathbf{S}^t\mathbf{V} \tag{5}$$

2.2. *Modeling of crystalline structure of DMW*

Several models of grain structures were proposed [13–17]. Among the models, Ogilvy's model [13] is widely used for

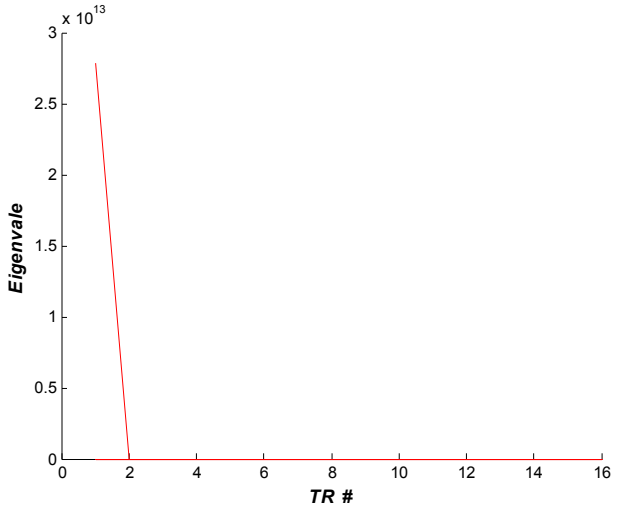

Fig. 3 – Eigenvalue of time reversal operator using the time reversal technique. TR, time reversal.

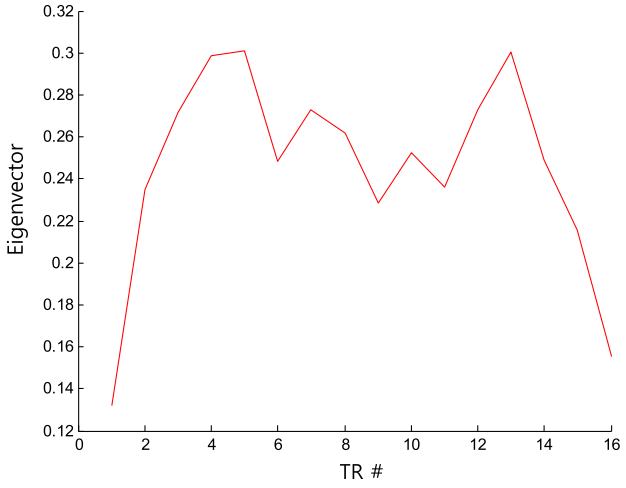

Fig. 4 – Eigenvector of time reversal operator using the time reversal technique.

describing grain structures in austenitic steel welds. Even though Ogilvy's model is widely used in the austenitic stainless steel welds, it can only describe symmetric welds. Therefore, it cannot be applied to the DMWs; in order to overcome this limitation, Ye et al [7] proposed a modified Ogilvy's model that can describe an unsymmetrical weld using Equations 6 and 7. In order to evaluate grain orientation in DMWs, the length of bottom line in weldments (D_1, D_2) and angle of weldments (α_1, α_2), as shown in Fig. 5, were measured. T_1 and T_2 are proportional to the tangents of the grain axes at the sloping edges in Fig. 5. Eta (η) is a parameter for determining how fast the grain orientation falls with an increase in y, varied between 0 and 1.

$$F(y,z) = \tan\theta_1 = \frac{(T_1(D_1 + z\tan\alpha_1))}{y^{\eta}} \quad y>0 \tag{6}$$

$$F(y,z) = \tan\theta_2 = \frac{(T_2|(D_2 + z\tan\alpha_2)|)}{|y^{\eta}|} \quad y<0 \tag{7}$$

D1, D2, α1, α2 can be obtained using actual weld geometry. Grain orientation in DMWs using T = 0.3 and η = 0.85 is

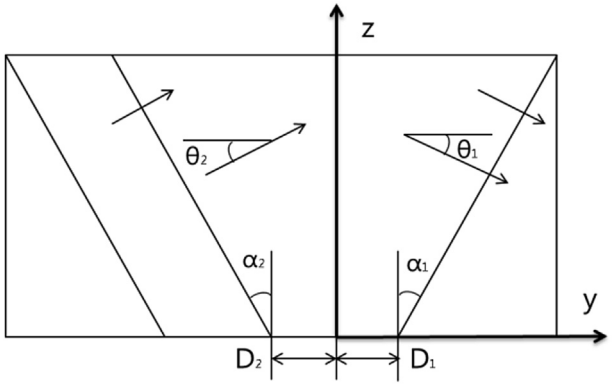

Fig. 5 – Geometry of modeling of the crystalline structure of dissimilar metal welds [17].

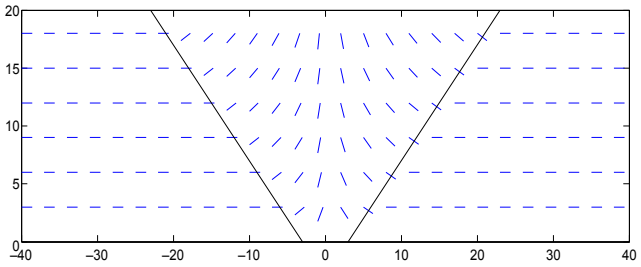

Fig. 6 – Calculation of the elastic constant for dissimilar metal welds.

calculated. Fig. 6 shows the result of grain orientation in DMWs based on the modified Ogilvy's model [17]. The basic elastic constants of transversely isotropic austenitic weld metal used, prior to rotation, are C11 = C22 = 241.1 GPa, C12 = C21 = 96.92 GPa, C13 = C23 = C31 = C32 = 138.03 GPa, C33 = 240.12 GPa, C44 = C55 = 112.29 GPa, and C66 = 72.09 GPa. The rotation matrix to elastic constant of transversely isotropic austenitic weld metal is applied, and then the elastic constant for applying to the simulation can be calculated using Equation 8.

$$G(\theta) = R(\theta)C_{ijkl} = \begin{bmatrix} \cos^2\theta & \sin^2\theta & 0 & 0 & 0 & \sin 2\theta \\ \sin^2\theta & \cos^2\theta & 0 & 0 & 0 & -\sin 2\theta \\ 0 & 0 & 1 & 0 & 0 & 0 \\ 0 & 0 & 1 & con\theta & -\sin\theta & 0 \\ 0 & 0 & 0 & \sin\theta & con\theta & 0 \\ \frac{-\sin\theta}{2} & \frac{\sin\theta}{2} & 0 & 0 & 0 & con2\theta \end{bmatrix} \times \begin{bmatrix} C_{11} & C_{12} & C_{13} & 0 & 0 & 0 \\ C_{12} & C_{22} & C_{23} & 0 & 0 & 0 \\ C_{13} & C_{23} & C_{33} & 0 & 0 & 0 \\ 0 & 0 & 0 & C_{44} & 0 & 0 \\ 0 & 0 & 0 & 0 & C_{44} & 0 \\ 0 & 0 & 0 & 0 & 0 & \frac{C_{11}-C_{12}}{2} \end{bmatrix} \tag{8}$$

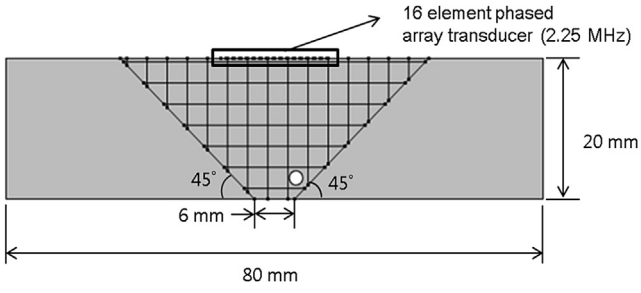

Fig. 7 – Finite element method setup of ultrasonic beam propagation.

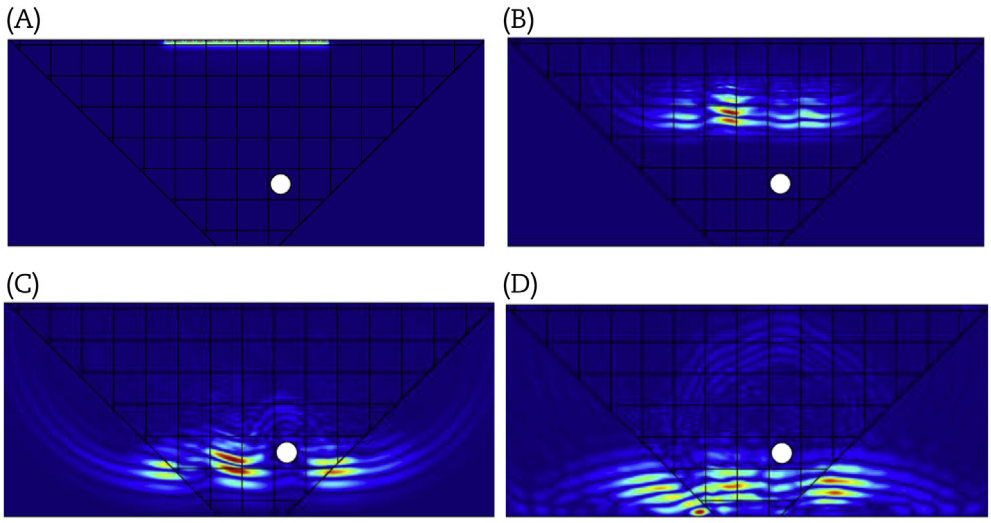

Fig. 8 – Simulation of phased array ultrasonic beam without time delay. (A) 0.5 μs, (B) 2.5 μs, (C) 3.5 μs, and (D) 5 μs.

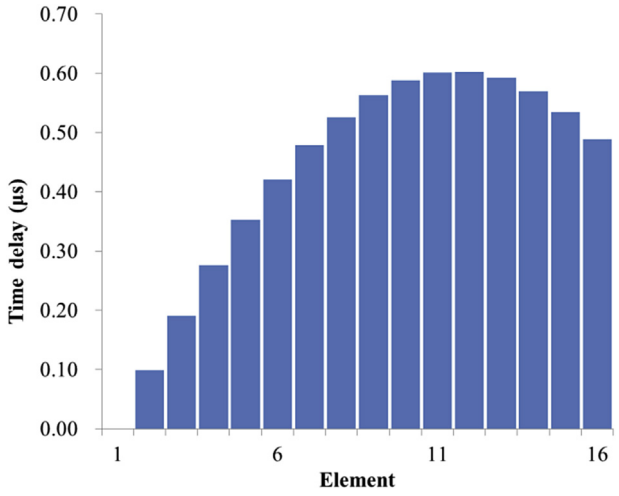

Fig. 9 – Calculated time delay using conventional focusing technique.

3. Results

3.1. *Simulation results*

To investigate the performance of the three focusing techniques for phased array ultrasonic testing in DMWs, firstly, simulating the ultrasonic beam propagation without a time delay was performed. The center frequency of transducer 2.25 MHz and 16 elements of phased array transducer are used. The width and spacing of the phased array transducer are 0.8 mm and 1 mm, respectively. Fig. 7 shows the simulation setup for ultrasonic propagation in DMWs. The calculations were carried out by a finite element modeling software, COMSOL Multiphysics. Simulation of ultrasonic beam propagation was applied to an acoustic–solid interaction model.

Fig. 8 shows a snapshot of simulated phased array ultrasonic beam without a time delay in the DMWs. As shown in Fig. 8, due to the complexity of grain orientation in weldments, it caused a beam distortion and skewing during

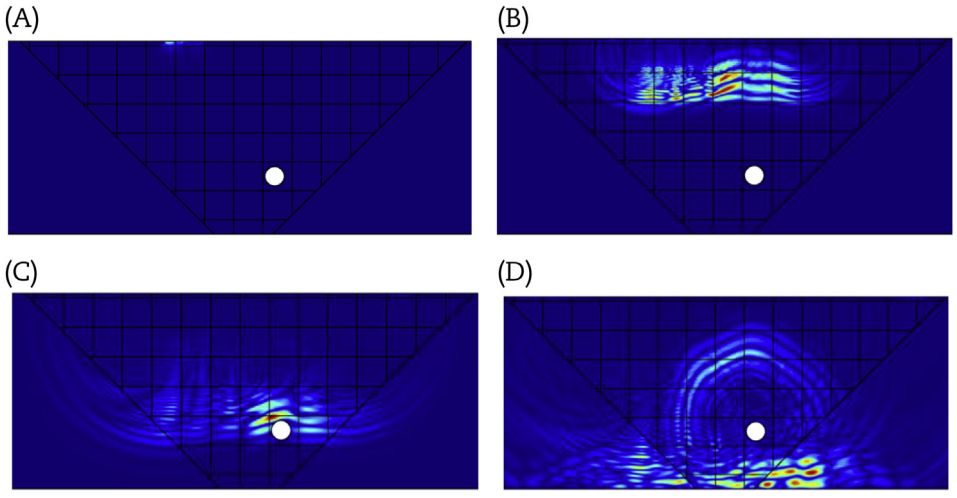

Fig. 10 – Simulation of ultrasonic beam propagation using conventional focusing technique. (A) 0.2 μs, (B) 1 μs, (C) 3 μs, and (D) 5 μs.

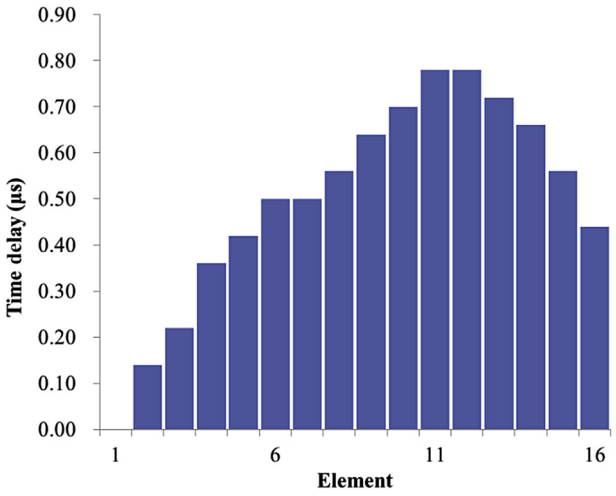

Fig. 11 – Calculated time delay using adaptive focusing technique.

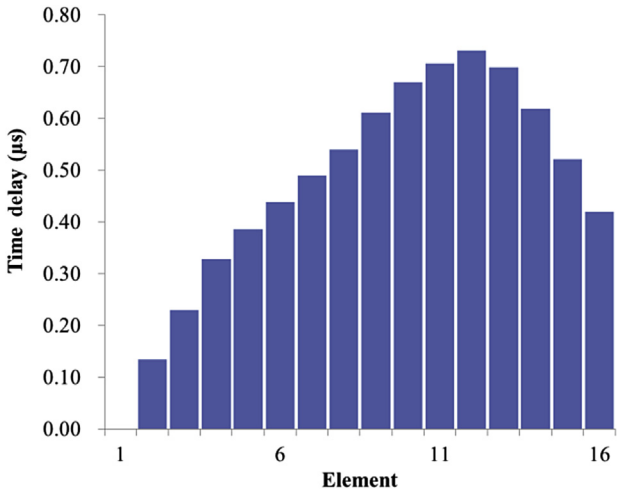

Fig. 13 – Calculated time delay using time reversal technique.

ultrasonic beam propagation. One can recognize a low signal–noise ratio from a side-drilled hole in weldments due to beam distortion and skewing. It is difficult to discriminate the flaw from the signals. For that reason, it is necessary to have enhanced focusing techniques to improve the signal–noise ratio. So, focusing techniques such as the time reversal technique and adaptive focusing technique were applied.

Fig. 9 shows the calculated time delay using Equation 3; relative time delay from each element is calculated. Fig. 10 shows a snapshot of simulated ultrasonic beam propagation using geometrical focusing techniques in DMWs. As shown in Fig. 10, the reflected beam from a side-drilled hole was not strong enough to clearly distinguish the flaw signal to noise signal. Using the geometrical focusing techniques, it still caused a beam distortion and skewing during the ultrasonic beam propagation.

Fig. 11 shows the calculated time delay using adaptive focusing techniques. Fig. 12 shows the simulation of ultrasonic beam propagation using adaptive focusing techniques. As shown in Fig. 12, the reflected beam from a side-drilled hole using the adaptive focusing technique was stronger than the reflected beam using the conventional focusing technique. Using the adaptive focusing technique, the beam distortion and skewing during ultrasonic beam propagation noticeably decreased compared to the conventional focusing technique.

Fig. 13 shows the calculated time delay using time reversal techniques. Fig. 14 shows the simulation of ultrasonic beam propagation using the time reversal technique. The reflected beam from a side-drilled hole using time reversal techniques was strongest among the focusing techniques. Using the time reversal technique, the beam distortion and skewing during the ultrasonic beam propagation noticeably decreased

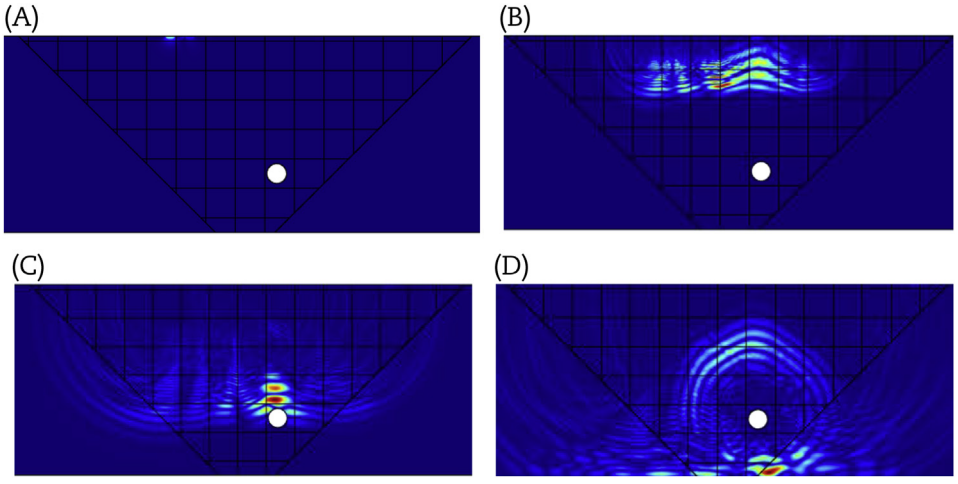

Fig. 12 – Simulation of ultrasonic beam propagation using adaptive focusing technique. (A) 0.2 μs, (B) 1 μs, (C) 3 μs, and (D) 5 μs.

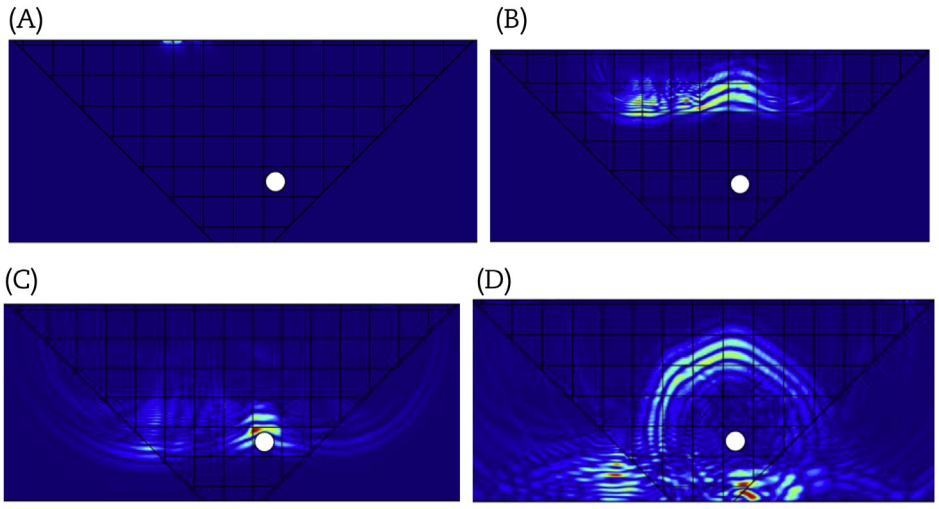

Fig. 14 – Simulation of ultrasonic beam propagation using a time reversal technique. (A) 0.2 μs, (B) 1 μs, (C) 3 μs, and (D) 5 μs.

compared to the conventional focusing technique and the adaptive focusing technique.

3.2. *Comparison of focused signals*

Fig. 15 shows the time delays that were calculated using three focusing techniques, and Fig. 16 shows the comparison of A-scan signals obtained by using the three different focusing techniques. For the conventional focusing technique, the amplitude of signal is the lowest. With the adaptive focusing technique, the amplitude is 64% higher than that obtained by the conventional focusing technique. When the time delay is determined by the time reversal techniques, the signal amplitude is the highest; 84% higher than that by the conventional one. Time reversal techniques enhanced Signal to Noise Ratio (SNR) of phased array ultrasonic signals most effectively compared to other techniques. Fig. 17 shows comparison of the signal amplitude obtained by three different focusing techniques.

4. Discussion

In this paper, performance of the three techniques, the conventional focusing technique, the adaptive focusing technique and the time reversal technique, in DMWs were investigated by comparison of scattered phased array ultrasonic signals from the Side Drilled Hole (SDH). In order to compare the focusing signals, simulation based approaches using commercial FEM software have been adopted. Crystalline structures of the DMWs were described by using the modified Ogilvy's. Furthermore, time delays for focusing phased array ultrasonic beams at the desired position in the

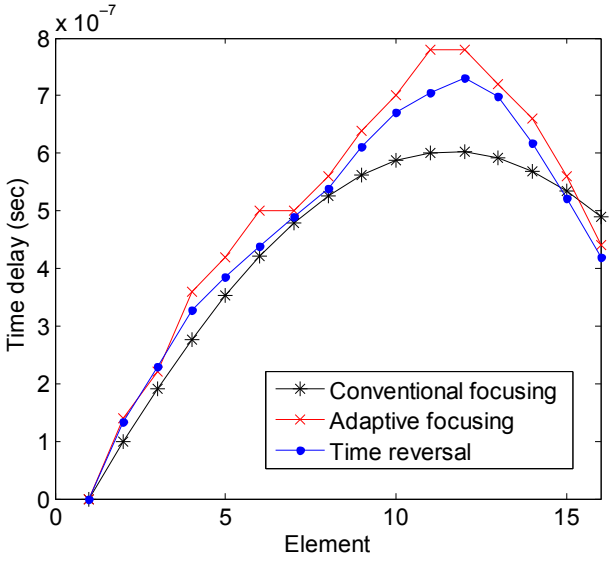

Fig. 15 – Calculated time delay using focusing techniques.

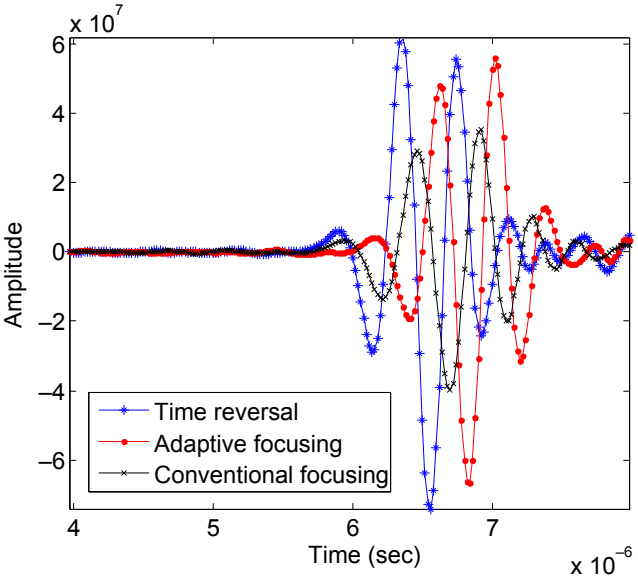

Fig. 16 – Comparison results of A-Scan signal using focusing techniques.

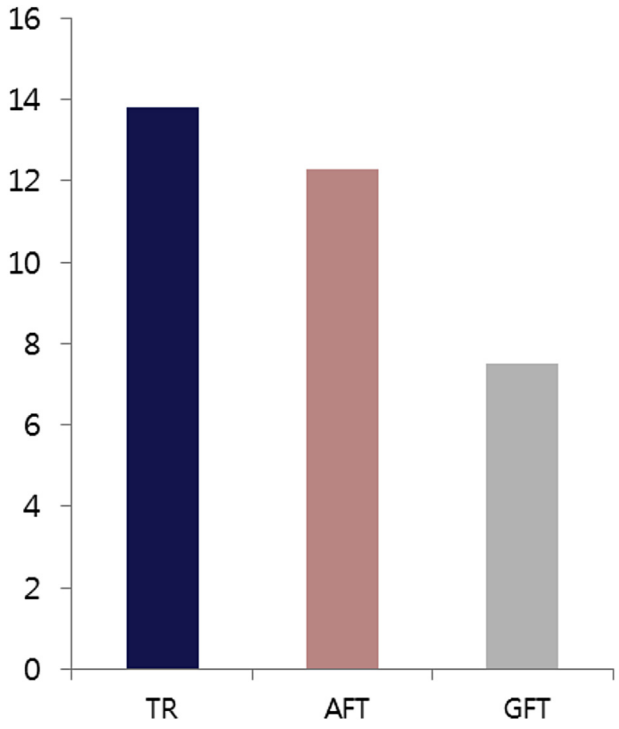

Fig. 17 – Amplitude of flaw signals using focusing techniques. AFT, Adaptive Focusing Technique; GFT, General Focusing Technique; TR, Time Reversal.

DMWs using three different focusing techniques were calculated. Then, comparisons of the predicted phased array ultrasonic signals using the calculated time delays were performed. Based on comparison results, time reversal technique shows better focusing performance of phased array ultrasound in the DMWs compare to the other two methods. However, both time reversal techniques and adaptive focusing techniques could be used for focusing ultrasound in DMWs.

Conflicts of interest

The authors declare no conflicts of interest.

Acknowledgments

This work was supported by the National Research Foundation of Korea (NRF) grant funded by the Korean government (MEST, No. 2012R1A1A2044423).

REFERENCES

[1] W. Bamford, J. Hall, A review of Alloy 600 cracking in operating nuclear plants including Alloy 82 and 182 weld behavior, in: 12th International Conference on Nuclear Engineering, 2004, pp. 131–139.
[2] V.V. Satyanarayana, G. Madhusudhan Reddy, T. Mohandas, Dissimilar metal friction welding of austenitic–ferritic stainless steels, J. Mater Process Tech. 160 (2005) 128–137.
[3] E. Becache, P. Joly, C. Tsogka, Application of the fictitious domain method to 2D linear elastodynamic problems, J. Comput. Acoust. 9 (2001) 1175–1202.
[4] B. Chassignole, D. Villard, M. Dubuguet, J.C. Baboux, R. El Guerjouma, Characterization of austenitic stainless steel welds for ultrasonic NDT, Rev. Prog. QNDE 20 (2000) 1325–1332.
[5] J. Moysan, A. Apfel, G. Corneloup, B. Chassignole, Modelling the grain orientation of austenitic stainless steel multipass welds to improve ultrasonic assessment of structural integrity, Intl J Press Vessel Piping 80 (2003) 77–85.
[6] J. Ye, H.J. Kim, S.J. Song, M.H. Song, S.C. Kang, S.S. Kang, K.C. Kim, Determination of focal laws for ultrasonic phased array testing of dissimilar metal welds, J. Korean Soc. Nondestructive Test. 28 (2008) 247–435.
[7] J. Ye, H.J. Kim, S.J. Song, S.S. Kang, K.C. Kim, M.H. Song, Model-based simulation of focused beam fields produced by a phased array ultrasonic transducer in dissimilar metal welds, NDE&E Int. 44 (2011) 290–296.
[8] S. Mahaut, J.-L. Godefroit, O. Roy, G. Cattiaux, Application of phased array techniques to coarse grain components inspection, Ultrasonics 42 (2004) 791–796.
[9] P. Calmon, D. Premel, Integrated NDT models in CIVA.
[10] S. Mahaut, S. Lonne, L.D. Roumilly, Validation of CIVA simulation tools for ultrasonic inspection in realistic configuration, ECNDT, 2006.
[11] N. Shafiza Mohd Tamim, F. Ghani, Techniques for optimization in time delay estimation from cross correlation function, Int. J. Eng. Technol. IJET-IJENS 10 (2010) 69–75.
[12] C. Prada, E. Kerbrat, D. Cassereau, M. Fink, Time reversal techniques in ultrasonic nondestructive testing of scattering media, Inverse Probl. 18 (2002) 1761–1773.
[13] J.A. Ogilvy, Computerized ultrasonic ray tracing in austenitic steel, NDT Int. 18 (1985) 66–67.
[14] J.A. Ogilvy, Ultrasonic beam profiles and beam propagation in an austenitic weld using a theoretical ray tracing model, Ultrasonics 24 (1986) 337–347.
[15] J.A. Ogilvy, Ultrasonic reflection properties of planar defects within austenitic welds, Ultrasonics 26 (1988) 318–327.
[16] J.A. Ogilvy, A layered media model for ray propagation in anisotropic inhomogeneous materials, Appl. Math. Model. 14 (1990) 237–247.
[17] J.A. Ogilvy, An iterative ray tracing model for ultrasonic nondestructive testing, NDT E Int. 25 (1992) 3–10.